Available online at www.sciencedirect.com
ScienceDirect
Journal of the European Ceramic Society 27 (2007) 3959–3962
www.elsevier.com/locate/jeurceramsoc

Properties variation of Bi-2212 directionally solidified induced by 0.4Pb substitution

M. Mora [a,*], A. Sotelo [a], H. Amaveda [a], M.A. Madre [a], J.C. Diez [a], F. Capel [b], J.M. López-Cepero [c]

[a] *Instituto de Ciencia de Materiales de Aragón, C.S.I.C., Universidad de Zaragoza, María de Luna, 3, 50018 Zaragoza, Spain*
[b] *Instituto de Cerámica y Vidrio, C.S.I.C. Campus de Cantoblanco, 28049 Madrid, Spain*
[c] *Departamento de Física de la Materia Condensada, Universidad de Sevilla, Apdo. 1065, 41080 Sevilla, Spain*

Available online 29 March 2007

Abstract

Vitreous cylinders with compositions $Bi_{2-x}Pb_xSr_2CaCu_2O_y$ ($x = 0$ and 0.4) were prepared and used as precursors to fabricate textured bars through a laser floating zone melting method (LFZ). The resulting textured cylindrical bars, after annealing, were electrical and mechanically characterized through resistivity as a function of temperature, *E–I* characteristics at 77 K, mechanical strength, σ, Young modulus, E_Y, Vickers hardness, H_v, and Weibull parameters, S_0 and m. The study of the mechanisms controlling the fracture process was made by means of the fractographical analysis using laser scanning confocal microscopy (LSCM). It has been found that the Pb addition lead to an increase of the slope of the *E–I* curves and to a change in the fracture mode.

Keywords: Laser zone melting; Mechanical properties; Superconductivity; Oxide superconductors

1. Introduction

One of the most attractive applications of $Bi_2Sr_2CaCu_2O_{8+\delta}$ (Bi-2212) superconductors is their use in fault current limiters,[1] providing the possibility to develop resistive-type fault current limiters. These would require the fabrication of Bi-2212 materials capable of supporting high critical current densities in the superconducting state and developing high resistance in the normal state, to effectively limit the fault current. However, the successful use of Bi-2212 superconducting ceramic materials as current limiters is conditioned by the low slope of the *E–I* curves obtained in the transition from the normal to the superconducting state. One solution to overcome this problem is based on the cationic substitution, which could introduce effective flux pinning centers and increase the slope of the *E–I* curves. In particular, the partial Bi substitution with Pb has shown to be useful to increase the intragranular pinning properties in single crystals, leading to the enhancement of both irreversibility field and critical current density.[2,3] Also, it has been demonstrated that Bi superconductors improve their electrical properties when they are properly processed.[4,5]

In this work, textured materials with compositions $Bi_2Sr_2CaCu_2O_{8+\delta}$ and $Bi_{1.6}Pb_{0.4}Sr_2CaCu_2O_{8+\delta}$, have been prepared using the laser floating zone melting method (LFZ). On these samples, the changes on the electrical as well as the mechanical properties have been studied through resistivity as a function of temperature, $\rho(T)$, *E–I* characteristics at 77 K, mechanical strength, σ, Young modulus, E_Y, Vickers hardness, H_v and Weibull parameters. Finally, the study of the mechanisms controlling the fracture process was made by means of the fractographical analysis, using laser scanning confocal microscopy (LSCM).[6] All these properties have been correlated with the Pb content.

2. Experimental

$Bi_{2-x}Pb_xSr_2CaCu_2O_{8+\delta}$, with $x = 0$ and 0.4 have been prepared from commercial Bi_2O_3 (Panreac, >98%), PbO (Panreac, >99%), $SrCO_3$ (Panreac, >98%), $CaCO_3$ (Panreac, >98.5%) and

* Corresponding author. Tel.: +34 976 762526; fax: +34 976 761957.
E-mail address: mmora@unizar.es (M. Mora).

0955-2219/$ – see front matter © 2007 Elsevier Ltd. All rights reserved.
doi:10.1016/j.jeurceramsoc.2007.02.128

CuO (Panreac, >97%) powders. They were weighted in the adequate atomic proportions, mixed in a ball mill and thermal treated twice under air (12 h at 750 and 780 °C) to decompose the carbonates and decrease the volume of the mixture. The pre-reacted mixture was melted at 1050 °C to assure good homogeneity and fluidity of the liquid, and then quenched into silica tubes, 2 mm inner diameter, to obtain long (more than 20 cm) and homogeneous cylindrical bars.[7]

The obtained cylinders were processed with a LFZ technique, described elsewhere.[8] In this process, the precursor bars are melted by the incidence of a Nd:YAG laser (1064 nm) under air. This melt is directionally solidified, at a growth rate of 40 mm/h, obtaining rods with a highly oriented microstructure. In order to obtain the appropriate phase composition (Bi,Pb)-2212, the as grown samples were annealed at 835 °C 60 h, followed by 12 h at 800 °C and quenched to room temperature.

The *E–I* characteristics at 77 K of the rods have been measured on 4 cm length samples by the standard four-probe configuration. From these measurements, the slope of the *E–I* curves has been determined, in the range of 1–20 μV/cm, using the power law $E \sim I^n$. Resistivity was measured from 77 to 300 K, using a dc current of 1 mA. From these measurements the critical temperature, T_c, was determined.

The mechanical strength was performed on a four-point bending apparatus. The tests were made at a loading rate of 0.5 mm/min. To determine E_Y, the deflection measurements in flexural strength test were used. H_v was determined by means of indentation tests in a Leco microhardness tester, with an applied load of 9.8 N for 15 s.

To characterize the fracture of the samples, the failure strength data were analyzed using the Weibull approach[9]:

$$\ln \ln \left[\frac{1}{1-\phi}\right] = m \ln \sigma - m \ln S_0 \quad (1)$$

where ϕ is the probability of failure, and S_0 and m are the scale and the shape parameters, respectively.

Fractographical studies of the different samples were performed using a Leica TCS-SP2 confocal microscope. The images were acquired in reflection mode, with a blue Ar laser (488 nm) as light source. The objectives used were 10× air (for the global views) and 20× air (for the detail views), which have 1.5 mm and 750 μm, respectively, as maximum lateral field of view. Typically, about 250 images were acquired for each height map, with 1–2 μm height steps.

Polished samples were examined in a scanning electron microscope (JEOL JSM 6400), in order to examine the texture.

3. Results and discussion

Fig. 1 shows SEM micrographs of the as grown samples, where black contrast phases are Bi-free secondary phases, and gray contrasts are related to Bi rich phases (Bi-2201 and Bi-2212). Usually, in the as grown samples, the texture can be reflected trough the black phases orientation (primary solidification phase)[10]. In this figure, it can be observed that the orientation of these phases is better for pure than for the Pb doped sample. Moreover, Pb addition disturbs the crystal growth habit, leading also to the misorientation of the Bi rich crystals (gray contrast). This effect is shown in Fig. 1, where the undoped sample exhibits the best texture, regarding Bi-rich phases (Fig. 1A), while Pb doped sample presents a misalignment of these phases (Fig. 1B).

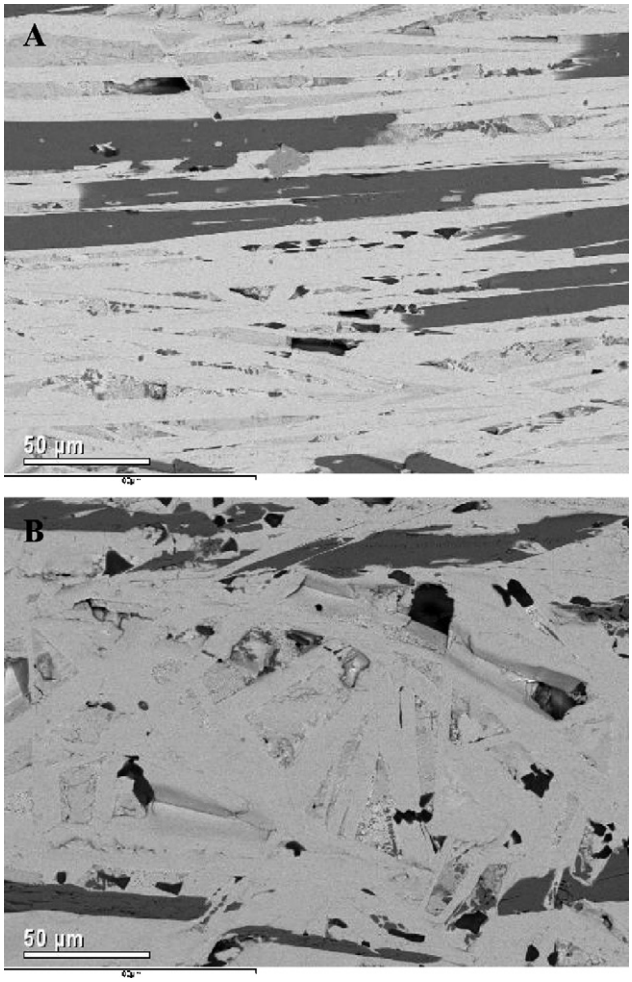

Fig. 1. Longitudinal SEM micrographs, showing the central view of the as grown samples for $Bi_2Sr_2CaCu_2O_{8+\delta}$ (A) and $Bi_{1.6}Pb_{0.4}Sr_2CaCu_2O_{8+\delta}$ (B). Bi-free phases are shown as black contrast.

After annealing, all the samples exhibit superconducting behavior as it is shown in Fig. 2, where resistivity as a function of temperature is displayed. However, the Pb addition leads to a decrease of T_c, from 90 to 86 K. On the contrary, Pb doping increases significantly the slope of the *E–I* curves. Typical *E–I* curves are plotted in Fig. 3 for pure and 0.4Pb doped samples. To clarify the graphical representation normalized current has been used and fitted using the power law to determine the *n*-values. It should be noted that the *n* reflects the sharpness of the superconducting to normal transition. Therefore, for Pb doped samples this transition is sharper ($n \sim 17$) than for pure samples ($n \sim 6$). Typical values for Bi-2212 are lower than 10, while for Bi-2223 can reach values as high as 20. It is clear that for LFZ textured samples with Pb content of 0.4 the obtained *n*-values are higher than those found for Bi-2212 and they are in the range of Bi-2223. This effect has been associated to the optimal Pb content inside of the Bi-2212 grains.[11]

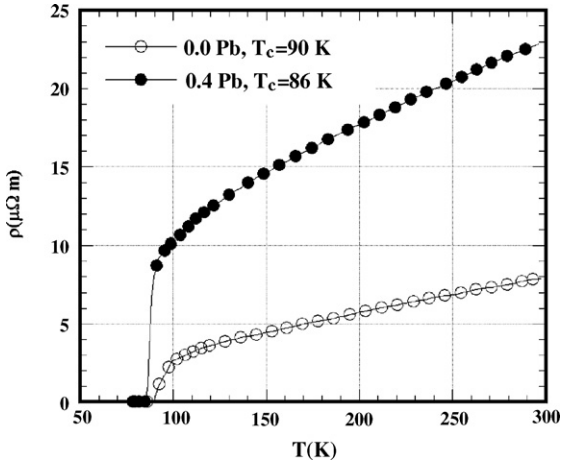

Fig. 2. Resistivity as a function of temperature for pure and Pb doped samples. Critical temperatures deduced from the curves are displayed.

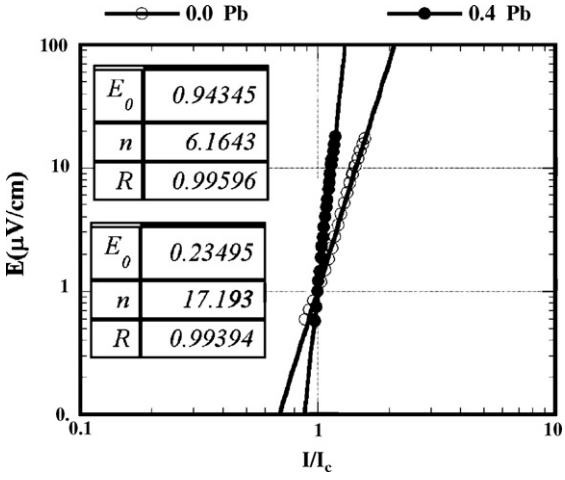

Fig. 3. Normalized fitted *E–I* curves between 1 and 20 microvolts/cm for pure and Pb doped samples. The *n*-values determined from the fitting are displayed.

The mechanical characteristics of the samples are resumed in Table 1, where the σ, E_Y, H_v and Weibull parameters are displayed. As can be seem from this table, the hardness of the Pb doped samples is higher than the undoped ones, due to the presence of bigger amount of secondary phases.[11] In both samples hardness measurements reveal that radial cracks were not formed. In pure samples the values obtained of σ and E_Y, are higher than the ones exhibited by the Pb doped. However, it is found a lower dispersion in measured values for the doped samples, as it is demonstrated by Weibull shape parameter (Table 1).

Table 1
Measured mechanical properties on doped and undoped samples

Sample	H_v (MPa)	σ_f (MPa)	E (GPa)	Weibull parameters	
				S_0	m
0.4Pb doped	295 ± 10	156 ± 10	75 ± 5	164	18.2
Undoped	205 ± 10	165 ± 30	85 ± 15	175	7.2

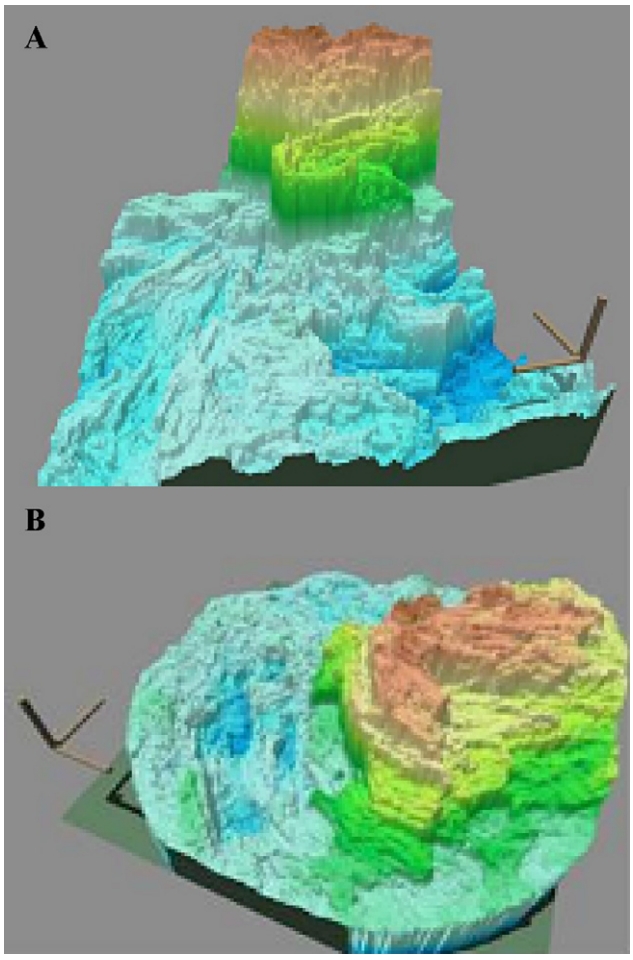

Fig. 4. 3D images of fracture surface of the undoped (A) and Pb doped sample (B) obtained from LSCM.

To illustrate the fracture characteristics, two representative fractured sample surfaces, doped and undoped, have been studied with LSCM. For each sample, two height maps (a global and a detail one), as well as 3D views and profiles of these height maps, have been acquired and calculated. The 3D image of fracture surface for undoped sample is displayed in Fig. 4A. Two main characteristics can be remarked. First, the visible "hill" at the center-right has very abrupt height changes, giving the sample a stairway-like appearance, with sharp "steps" separated by plateau-like regions with comparatively small roughness. The greater height difference is about 400 μm as obtained from the profiles of the height maps. Second, the whole surface of the sample has a texture, which could be described as "fibrous", with prominent linear features that also show the step-plateau behavior of the main hill, in a less pronounced way.

When comparing the fracture surface of the Pb doped (Fig. 4B) with the undoped samples, some differences are easily noticeable. Firstly, the fracture surface shows a rougher look and is flatter than undoped one. The greater height difference in this case is about 250 μm. Secondly, the linear structures are less pronounced and more irregular than in the undoped one.

It is very clear that there is an underlying feature common to both samples, namely the "fibrous" texture. In the undoped case this texture is clearly defined, present throughout the whole surface, and is accompanied by abrupt height steps which give the surface a stair-like appearance. The high steps are indicative of a high amount of elastic energy accumulation just before fracture. In the Pb doped sample, however, the surface does not present abrupt height changes and the base texture is not as extended or well defined. These results, consequently, are in agreement with the microstructure of the doped and undoped samples shown in Fig. 1, and justify the mechanical behavior of the analyzed samples.

4. Conclusions

Bulk samples of Bi-2212 with compositions $Bi_2Sr_2CaCu_2O_{8+\delta}$ and $Bi_{1.6}Pb_{0.4}Sr_2CaCu_2O_{8+\delta}$, have been prepared and textured by a LFZ process. It has been found a more abrupt transition between the normal to superconductor state in the Pb doped samples, with *n*-values nearly three times higher than for the pure ones.

Lead addition eases fracture initiation and propagation, yielding fracture surfaces with less marked features and a flatter overall shape, leading to a decrease of σ and E_Y, which is in agreement with the microstructural analyses.

Acknowledgments

The authors are indebted to the Spanish Ministry of Education and Science (project MAT2005-06279-C03-01) and to the Aragon Regional Government (Consolidated Research Groups E03 and T12) for financial support.

References

1. Paul, W., Chen, M., Lakner, M., Rhyner, J., Braun, D. and Lanz, W., Fault current limiter based on high temperature superconductors—different concepts, test results, simulations, applications. *Physica C*, 2001, **354**, 27–33.
2. Chong, I., Hiroi, Z., Izumi, M., Shimoyama, J., Nakayama, Y., Kishio, K. *et al.*, High critical current density in the heavely Pb-doped $Bi_2Sr_2CaCu_2O_{8+\delta}$ superconductor: generation of efficient pinning centers. *Science*, 1997, **276**, 770–773.
3. Musolino, N., Bals, S., van Tendeloo, G., Clayton, N., Walker, E. and Flükiger, R., Modulation-free phase in heavely Pb-doped (Bi,Pb)2212 crystals. *Physica C*, 2003, **399**, 1–7.
4. Huang, Y., de la Fuente, G. F., Sotelo, A., Badía, A., Lera, F., Navarro, R. *et al.*, $(Bi,Pb)_2Sr_2Ca_2Cu_3O_{10+\delta}$ superconductor composites: ceramics vs. fibers. *Physica C*, 1991, **185–189**, 2401–2402.
5. Garnier, V., Caillard, R., Sotelo, A. and Desgardin, G., Relationship among synthesis, microstructure and properties in sinter-forged Bi-2212 ceramics. *Physica C*, 1999, **319**, 197–208.
6. Lopez-Cepero, J. M., Cancapa, J. J. Q., Lopez, A. R. D. and Fernández, J. M., Fractographic studies of sapphire fibers using laser scanning confocal microscopy. *Key Eng. Mater.*, 2005, **290**, 280–283.
7. Sotelo, A., Mora, M., Madre, M. A., Diez, J. C., Angurel, L. A. and Mayoral, M. C., Preparación y caracterización de vidrios cerámicos Bi-2212. In *Proceedings of VIII Congreso Nacional de Materiales*. Universidad Politécnica de Valencia, 2004. pp. 207–210.
8. de la Fuente, G. F., Diez, J. C., Angurel, L. A., Peña, J. I., Sotelo, A. and Navarro, R., Wavelength dependence in laser floating-zone processing: a case study with Bi-Sr-Ca-Cu-O superconductors. *Adv. Mater.*, 1995, **7**, 853–856.
9. Weibull, W., A statistical distribution function of wide applicability. *J. Appl. Mech. -Trans. ASME*, 1951, **18**, 293–297.
10. Costa, F. M., Silva, R. F. and Vieira, J. M., Diffusion phenomena and crystallization path during the growth of LFZ Bi-Sr-Ca-Cu-O superconducting fibres. *Supercond. Sci. Technol.*, 2001, **14**, 910–920.
11. Sotelo, A., Mora, M., Madre, M. A., Amaveda, H., Diez, J. C., Angurel, L. A. *et al.*, Study of the variation of the E-I curves in the superconducting to normal transition of Bi-2212 textured ceramics by Pb addition. *Bol. Soc. Esp. Ceram. V*, 2006, **45**, 228–232.